Antimycobacterial Activities of Hydroxamic Acids and Their Iron(Ii/Iii), Nickel(Ii), Copper(Ii) and Zinc(Ii) Complexes

Dong Yang , Yanfang Zhang , Ibrahima Sory Sow , Hongping Liang , Naima El Manssouri , Michel Gelbcke , Lina Dong , Guangxin Chen , François E. Dufrasne , Véronique Fontaine , Rongshan Li *

Posted Date: 4 September 2023

doi: 10.20944/preprints202309.0122.v1

Keywords: Hydroxamic acids; Antibacterial; Anti-biofilm; Mycobacterium tuberculosis

Article

Antimycobacterial Activities of Hydroxamic Acids and Their Iron(II/III), Nickel(II), Copper(II) and Zinc(II) Complexes

Dong Yang [1], Yanfang Zhang [1], Ibrahima Sory Sow [2], Hongping Liang [1], Naïma El Manssouri [2], Michel Gelbcke [2], Lina Dong [3], Guangxin Chen [4], François Dufrasne [2], Véronique Fontaine [2] and Rongshan Li [5]

[1] Clinical Laboratory, Shanxi Provincial People's Hospital, Affiliated of Shanxi Medical University, Taiyuan 030001, China; yangdcmu@163.com (D.Y.); ZhangYF2065@163.com (Y.F.Z.); sxrmyyjyk@163.com (H.P.L.);
[2] Microbiology, Bioorganic and Macromolecular Chemistry Unit, Faculty of Pharmacy, Université libre de Bruxelles (ULB), Boulevard du Triomphe, 1050 Brussels, Belgium; Ibrahima.Sory.Sow@ulb.be (I.S.S.); naima.el.manssouri@ulb.be (N.E.M.); michel.gelbcke@ulb.be (M.G.); francois.dufrasne@ulb.be (F.D.); veronique.fontaine@ulb.be (V.F.)
[3] Core Laboratory, Shanxi Provincial People's Hospital (Fifth Hospital) of Shanxi Medical University; Taiyuan 030012, China; donglina1983@126.com (L.N.D.);
[4] Institutes of Biomedical Sciences, Shanxi University, Taiyuan 030006, China; chengx@sxu.edu.cn (G.X.C.)
[5] Department of Nephrology, The Affiliated People's Hospital of Shanxi Medical University, Shanxi Provincial People's Hospital, Shanxi Kidney Disease Institute, Taiyuan 030001, China.
* Correspondence: rongshanli13@163.com

Abstract: Hydroxamic acid (HA) derivates displayed antibacterial and antifungal activities. HA with various numbers of carbon atoms (C_2, C_6, C_8, C_{10}, C_{12} and C_{17}), complexed to different metal ions Fe(II/III), Ni(II), Cu(II) and Zn(II) were evaluated for their antimycobacterial activities and their anti-biofilm activities. Some derivates, among others HA12Fe2, inhibited the development of *Mycobacterium tuberculosis*, *Mycobacterium bovis* BCG and *Mycobacterium marinum* biofilms and could even attack pre-formed *Pseudomonas aeruginosa* biofilm. Proteomic profiles showed that the potential targets of HA10FeCl were mainly related to mycobacteria stress adaptation, involving cell wall lipid biosynthesis, drug resistance and tolerance, siderophore metabolism. This study provides new insights regarding the antimycobacterial activities of the HA and their complexes, especially about their potential antibiofilm activities.

Keywords: Hydroxamic acids; Antibacterial; Anti-biofilm; *Mycobacterium tuberculosis*

1. Introduction

Tuberculosis (TB) is a communicable disease caused by the pathogenic bacillus *Mycobacterium tuberculosis*. According to the WHO Global Tuberculosis Report 2022, globally, in 2021, an estimated 10.6 million people developed an active tuberculosis and 1.58 million died from tuberculosis [1]. In addition, occurrence of increasing numbers of multi drug-resistant (MDR) and extensively drug-resistant (XDR) *Mycobacterium tuberculosis* strains is of great concern [1]. *Mycobacterium tuberculosis* cell wall contains from the inside to the outside, an arabinogalactan layer covalently attached to the peptidoglycan layer and mycolic acids, covalently attached to the arabinogalactan, in which various unique long carbon chain lipids can be further embedded. The complex outer membrane is further wrapped up by capsular and biofilm extracellular compounds [2]. Some of the long and complex lipids non-covalently attached to the outer membrane, only present in pathogenic mycobacteria, such as the phthiocerol dimycocerosate (PDIM), have been shown to play important roles, not only in virulence, *i.e.*, for camouflage in macrophages, but also in antibiotic intrinsic resistance [3,4]. Furthermore, pathogenic mycobacteria show slow growth, tending to enter in a non-replicative state when facing *in vivo* stress conditions, eventually leading to dormancy. To circumvent this metabolic characteristic, long (more than 6 months) and complex (more than 4 drugs) must be administrated to

 doi:10.20944/preprints202309.0122.v1

the patients in order to eradicate the infection. Despite the efficacy of the current anti-TB treatments, several factors, such as poor patient compliance, toxicity of drugs and irrational prescribing practices increase the risk of drug-resistant strain selection. This leads to even further difficult and more expensive treatment [1]. Thus, novel and efficient anti-tuberculosis drugs are urgently need to fight TB.

Since the first hydroxamic acid (HA) discovery in 1869, HA and its related analogs have been intensively studied. This chemical component class shows diverse applications, in biology, industry and medicine. Interestingly, some of the HA derivates displayed antimicrobial properties with anti-bacterial, anti-virulence or anti-fungal activities. For instance, the benzoylacetone and HA complexes could inhibit the *A. hydrophila*, *S. aureus*, *E. aerogenes*, *S. sonnei*, *P. aeruginosa*, *S. typhimurium*, *S. epidermidis*, and *M. luteus* [5]. Cyclic hydroxamic acid (*N*-hydroxylactam) able to chelated iron ions inhibited iron-containing enzyme lipoxygenase in Gram-negative *P. aeruginosa* [6]. Heterocyclic methylsulfone hydroxamates analogous inhibited the LpxC enzyme activity, involved in lipopolysaccharide (LPS) production of Gram-negative bacteria [7]. Due to the potential values of HA analogues in the field of medicine development, we previously synthesized various HA derivates, including complexes with varying numbers of carbon atoms (C_2, C_6, C_8, C_{10}, C_{12} and C_{17}) and their corresponding Fe(II/III), Ni(II), Cu(II) and Zn(II) complexes and we observed that the C_6 to C_{12} HA derivates complexed with Fe(II/III) had antibacterial activities against gram positive and negative bacteria while the C_{12} HA had a larger spectrum activities, on bacteria and yeast [8]. The C_{12} HA compounds complexed or not to the Fe(II/III) even showed an antimycobacterial activity on *M. smegmatis* [8].

Furthermore, HA analogs also displayed antimycobacterial activity against mycobacteria, like *M. tuberculosis*, *M. abscessus*, *M. marinum*, *M. smegmatis* [9–11]. The complexes of benzohydroxamate associated with transition metallic ions (Cu^{2+} and Co^{2+}) could inhibit *M. tuberculosis* growth by interaction with the urease in the nitrogen metabolism [9]. The compound of *para*-nitrobenzohydroxamic acid demonstrated a minimum inhibitory concentration (MIC) of 0.71 µM in glycerol-alanine salt medium or a MIC of 7.79 µM in 7H12 medium on *M. tuberculosis* [12]. The pentacyanoferrate moiety in Fe(II) coordination hydroxamic complexes benefited of the release of HNO from HA, improving pyrazinamide and delamanid efficiency against *M. tuberculosis* [13]. The suberoylanilide hydroxamic acid (SAHA) also had adjunctive potential to enhance the effects of first-line anti-TB drugs (isoniazid and rifampicin) against intracellular *M. tuberculosis* [14].

The aims of this study was to evaluate the potential and selective antimycobacterial and anti-biofilm activities (on *M. tuberculosis*, *M. bovis* BCG and *M. marinum*) of 47 HA derivates, containing various numbers of carbon atoms (C_2, C_6, C_8, C_{10}, C_{12} and C_{17}) and eventually complexed with Fe(II/III), Ni(II), Cu(II) and Zn(II), to further assess their potentials as anti-TB or anti-biofilm drug candidates.

2. Material and methods

2.1. Materials

The mycobacteria strains, including *M. bovis* BCG (Pasteur 1173P2), *M. tuberculosis* H37Ra, *M. marinum* (M strain) were obtained from Gene Optimal (Shanghai, China). The *P. aeruginosa* (LMG 6395) was purchased from Belgian Coordinated Collection of Microorganisms (BCCM), University of Gent. The 7H9 broth and OADC medium were purchased form BD (BD BBL™, USA). The Mueller Hinton broth (MHB) was purchased from Sigma- Aldrich (Saint Louis, USA). HA derivate stocks at 10 mM to 200 mM were prepared in DMSO or methanol.

2.2. Methods

2.2.1. Antimycobacterial drug susceptibility assay

Mycobacteria precultures were grown in 25 cm^2 flasks at 37°C without shaking in 7H9 medium (BD) supplemented with 10% (v/v) OADC (BD) to an OD_{600} of 0.7-0.9. The macrodilution method was

 doi:10.20944/preprints202309.0122.v1

performed in 10 mL screw tubes in 7H9 medium (BD) containing 0.05% glycerol and 10% OADC. Five hundred µL inoculum diluted in the supplemented 7H9 medium to reach an optical density at 600 nm (OD_{600}) of 0.01 were added to 500 µL serial drug dilutions in the same 7H9 medium. Tubes were placed without shaking at 37°C. Growth or absence of growth were recorded on the day that the growth of the 100-fold diluted drug-free inoculum control became visible in order to assess the minimal inhibitory concentration of the drugs (MIC, being the lowest drug concentration inhibiting more than 99% of mycobacteria growth)[15]. This experiment was performed three times to check the reproducibility of the MIC determination.

The combined effect of vancomycin and chemical component was also performed using microdilution method. The fractional inhibitory concentration index (FICI) was calculated according to the checkerboard method. $FICI=FIC_a+FIC_b=MIC_{ab}/MIC_a+MIC_{ba}/MIC_b$. MIC_a or MIC_b is the MIC of the chemical component or vancomycin alone, MIC_{ab} is the MIC of the chemical component in combination with a fixed vancomycin concentration, MIC_{ba} is the MIC of the vancomycin in combination with a fixed chemical component concentration were obtained. The fixed concentrations were 4 and 20-fold lower than the MIC_a or MIC_b, respectively. In agreement with the checkerboard method, synergy is reached when the FICI is < 0.5 [16].

2.2.2. Biofilm growth assay

For mycobacteria, precultures were grown in 7H9 medium with 10% (v/v) OADC to an optical density at 600 nm (OD_{600}) of 0.8-0.9. The biofilm growth inhibition assay was performed in the 6-well plate or 24-well plate in the Sauton's medium[17,18]. All the compound samples were first diluted within Sauton's medium to various concentrations. The mycobacteria precultures were inoculated as a 100-fold dilution (corresponding approximately to 9×10^5 CFU/mL inoculum) in the plates, giving a final culture volume of 4 mL or 2 mL, in the 6-well plate or 24-well plate, respectively. The plates were covered with two layers of Parafilm® "M" and incubated at 37 °C. Biofilm formation was visually assessed after 3-4 weeks of culture.

In contrast to the mycobacteria biofilm inhibition test, the *P. aeruginosa* biofilm inhibition test was performed on pre-formed biofilms[19]. *P. aeruginosa* pre-formed biofilms were obtained on the TSP (solid phase transfer) covers (Nunc) of the 96-well from a 10^6 CFU/mL starting inoculum incubated for 24 h in MHB. After 24 h, covers with pre-formed biofilms were immersed and incubated at 37 °C for twelve days in 100 µL of MHB containing compound samples at different concentrations ranging from between 20-2500 µM. Cetrimide was used as a control (concentrations between 78 ng/mL to 1 µg/mL). Biofilm control wells developed in the presence of 5% (v/v), DMSO or MeOH were present on each plate. The TSP coverslips containing the previously formed biofilm were used to cover the supports of the plates containing the test compound solutions. These plates were incubated at 37 °C for twelve days [19]. During the incubation period, observation of the plates was performed daily to ensure the presence of the MHB medium. The experiment was performed twice in triplicate for each solution of tested compounds.

2.3. Proteomic analysis

In order to identify potential targets of the HA complexes, we performed proteomic analysis. The *M. bovis* BCG (Pasteur 1173P2) strain was treated with HA10FeCl for 7 days and mycobacteria without HA10FeCl were used as control. The bacterial pellets were collected by centrifugation with 3000 g for 15 min and washed twice with cold PBS. Bacteria were resuspended and lysed in the SDT lysis buffer (4% m/v, SDS, 100 mM Tris-HCl pH7.6, 1 mM DTT). The extracted proteins were quantified with the BCA Protein Assay Kit (Bio-Rad, USA). Protein digestion by trypsin was performed according to filter-aided sample preparation (FASP) procedure [20]. The digested peptides of each sample were desalted on C18 Cartridges (Empore SPE cartridges, Sigma), concentrated by vacuum centrifugation and reconstituted in 40 µl of 0.1% (v/v) formic acid.

LC-MS/MS analysis was performed on a timsTOF Pro mass spectrometer (Bruker) that was coupled to Nanoelute (Bruker Daltonics) for 60/120/240 min. The peptides were loaded onto a reverse phase trap column (Thermo Scientific) connected to the C18-reversed phase analytical column

Preprints (www.preprints.org) | NOT PEER-REVIEWED | Posted: 4 September 2023 doi:10.20944/preprints202309.0122.v1

(Thermo Scientific Easy Column, 10 cm long, 75 µm inner diameter, 3 µm resin) in buffer A (0.1% formic acid) and separated with a linear gradient of buffer B (84% acetonitrile and 0.1% formic acid) at a flow rate of 300 nl/min. The mass spectrometer was performed in a positive ion mode. The mass spectrometer collected ion mobility MS spectra over a mass range of m/z 100-1700 and 1/k0 of 0.6 to 1.6, and then performed 10 cycles of PASEF MS/MS with a target intensity of 1.5 k and a threshold of 2500. Active exclusion was enabled with a release time of 0.4 minutes.

MS raw data were combined and searched using the MaxQuant software (version: 1.5.3.17) for identification and quantitation analysis and a UniProt *Mycobacterium bovis* (strain BCG/Pasteur 1173P2) database (https://www.uniprot.org/). The protein hits with a p value < 0.05 (*t* test) and a fold change <0.8 or >1.2 were further analysed.

3. Results

3.1. HA compounds present anti-mycobacterial activities

In order to identify whether the HA derivatives could have antimycobacterial activities, we assessed those activities in planktonic condition and in stress condition with high glycerol concentration leading to biofilm development. Biofilm conditions are indeed known to better mimic the stressful *in vivo* condition [21–23]. These antimycobacterial activities were assessed using three strains, harboring various characteristics, among others, the presence of absence of the phthiocerol dimycocerosate (PDIM) lipids in their cell wall: the H37Ra *M. tuberculosis* strain is PDIM negative and is a slow growing strain, the *M. marinum* is PDIM positive and a slow growing mycobacteria (however in planktonic culture it grows faster than *M. bovis* BCG or H37Ra *M. tuberculosis* strains) and the *M. bovis* BCG is PDIM positive and a slow growing mycobacteria. The drug susceptibility assays performed under planktonic growth condition eventually allowed to identify the minimal inhibitory concentration (MIC), while those performed under biofilm growth development allowed to eventually identify the minimal biofilm-formation inhibitory concentration (MBIC).

In planktonic conditions, various HA and complexes displayed anti-mycobacterial activities, especially on *M. tuberculosis* H37Ra strain (Tables 1–3). The active compounds had generally a MIC ≥ 200 µM on the three species. An inhibitory activity was less often observed on *M. marinum*, with only the HA10 and the HA8FeCl and HA8Fe3 complexes showing an anti-mycobacterial activity. On the *M. bovis* BCG, 8 compounds showed an inhibitory activity, however with relatively high MIC (≥ 200 µM), except for HA10FeCl showing a MIC of 100-200 µM.

Table 1. MIC and MBIC values (µM) of HA iron complexes against *M. bovis*, *M. marinum* and *M. tuberculosis*.

Compound	*M. bovis* BCG		*M. marinum*		*M. tuberculosis* H37Ra	
	MIC	MBIC	MIC	MBIC	MIC	MBIC
	µM	µM	µM	µM	µM	µM
HA2FeCl	> 500	**500**	> 500	**250**	> 500	**250**
HA6FeCl	> 500	**300**	> 500	≥ 250	**500**	**125**
HA8FeCl	≥ 500	**100**	**200**	**62.5**	**500**	**250**
HA10FeCl	**100-200**	**20-100**	> 200	**62.5**	**125**	**31.25**
HA12FeCl	> 200	**100**	> 200	**500**	**125**	**125**
HA17FeCl	> 500	> 500	> 500	**500**	**250**	> 500
HA2Fe2	> 500	> 500	> 500	> 500	> 500	> 500
HA6Fe2	> 500	**100-500**	> 500	**500**	**500**	**250**
HA8Fe2	> 500	**100-200**	> 500	**500**	**500**	**250**
HA10Fe2	> 200	**20**	> 200	> 500	**250**	> 500
HA12Fe2	> 500	**100**	> 500	> 500	**500**	**500**
HA17Fe2	**250**	> 500	> 500	500	**125**	**250**
HA2Fe3	**250-500**	**300-500**	> 500	**250**	> 500	**125**
HA6Fe3	**500**	**100-500**	> 500	**250**	≥ 500	**62.5-125**

Preprints (www.preprints.org) | NOT PEER-REVIEWED | Posted: 4 September 2023 doi:10.20944/preprints202309.0122.v1

HA8Fe3	**500**	**100**	**250-500**	≥ 125	**125**	**31.25**
HA10Fe3	≥ 200	**20-40**	> 200	**62.5**	**125**	**31.25-62.5**
HA12Fe3	≥ 200	**100**	> 200	**200-500**	**125-250**	**125**
HA17Fe3	> 200	> 500	> 500	**200-500**	**125**	**62.5**

HA= hydroxamic acid, HAnFe2= iron(II) complexes, HAnFeCl= iron(III) complexes with n=2, 6, 8, 10, 12 and 17 (carbon chain).

Table 2. MIC and MBIC values (μM) of zinc, nickel(II) and copper(II) complexes against *M. bovis* BCG, *M. marinum* and *M. tuberculosis*.

Compound	*M. bovis* BCG		*M. marinum*		*M. tuberculosis* H37Ra	
	MIC	MBIC	MIC	MBIC	MIC	MBIC
	μM	μM	μM	μM	μM	μM
HA2Zn2	> 500	> 500	> 500	**500**	> 500	**250**
HA6Zn2	> 500	**200**	> 500	**500**	**125**	**125**
HA8Zn2	> 500	**100-200**	> 500	**500**	**250**	**250**
HA10Zn2	**250**	**100**	**250**	**250-500**	**250**	**250**
HA12Zn2	> 500	**100**	> 500	**250**	**250**	**125**
HA17Zn2	> 500	> 500	> 500	**500**	> 500	**250**
HA2Ni2	> 500	**300-500**	> 500	> 500	> 500	**62.5-125**
HA6Ni2	> 500	**200**	> 500	**500**	> 500	**31.25**
HA8Ni2	> 500	**100**	> 500	**62.5**	> 500	**31.25**
HA10Ni2	> 200	**20**	> 200	**500**	**500**	**125**
HA12Ni2	> 500	**100**	> 500	**125**	> 500	**250-500**
HA17Ni2	> 500	> 500	> 500	**250**	> 500	**250**
HA2Cu2	**250-500**	**300**	> 500	≥ 250	≥ 500	**250**
HA6Cu2	≥ 500	**100**	> 500	**500**	> 500	**500**
HA8Cu2	> 200	**100-200**	> 200	**250**	> 500	**250**
HA10Cu2	> 200	**20**	> 200	**250**	**250**	**250**
HA12Cu2	> 500	**100**	> 500	**125**	> 500	**250**
HA17Cu2	> 500	≥ 500	> 500	≥ 500	> 500	**250**

HAZn2=zinc complexes, HAnNi2= nickel(II) complexes, HAnCu2= copper(II) complexes with n=2, 6, 8, 10, 12 and 17 (carbon chain).

Table 3. MIC and MBIC values (μM) of HA complexes, iron(II)-, iron(III)-, nickel(II)-, copper(II)-, zinc(II)- chloride against *M. bovis*, *M. marinum* and *M. tuberculosis*.

Compound	*M. bovis* BCG		*M. marinum*		*M. tuberculosis* H37Ra	
	MIC	MBIC	MIC	MBIC	MIC	MBIC
	μM	μM	μM	μM	μM	μM
HA2	> 500	> 500	> 500	**500**	> 500	**250**
HA6	> 500	**~ 100**	> 500	**500**	**500**	**125**
HA8	> 500	**100**	> 500	**500**	**500**	**125**
HA10	**250-500**	**100**	**250-500**	**250**	> 500	**125**
HA12	> 500	**100-500**	> 500	> 500	**125**	**250**
HA17	> 500	> 500	> 500	≥ 500	≥ 500	> 500
$FeCl_2$	> 500	> 500	> 500	**500**	> 500	> 500
$FeCl_3$	> 500	> 500	> 500	**500**	> 500	> 500
$NiCl_2$	> 200	> 500	**500**	≥ 500	> 500	**250**
$CuCl_2$	> 200	**200**	> 200	**250**	> 500	**500**
$ZnCl_2$	> 500	> 500	> 500	**250**	> 500	**125-250**

HA complexes with n=2, 6, 8, 10, 12 and 17 (carbon chain).

Preprints (www.preprints.org) | NOT PEER-REVIEWED | Posted: 4 September 2023 doi:10.20944/preprints202309.0122.v1

In stressful condition, mycobacteria were grown into biofilm. Biofilm formation was visible from 10-12 days for *M. bovis* BCG and *M. tuberculosis* H37Ra, from 15-20 days for *M. marinum* and mature biofilms were obtained in 20-24 days for *M. bovis* BCG, in 28-30 days for H37Ra *M. tuberculosis* and in 35-40 days for *M. marinum*. The biofilm was thinner for *M. marinum*, compared to those of *M. bovis* BCG and H37Ra *M. tuberculosis*. Again, more compounds had biofilm inhibitory activities on the H37Ra *M. tuberculosis* strain. The HA10 was active on the three biofilms with minimal biofilm-formation inhibitory concentration (MBIC) ranging between the 100 and 250 µM, depending on the bacteria strain. For most active compounds on the *M. marinum* biofilm, the MBIC were ≥ 200 µM, except for HA8FeCl, HA10FeCl, HA10Fe, HA8Ni2 with MBIC of 62.5 µM and for HA12Ni2 and HA12Cu2 with MBIC of 125 µM. For *M. bovis* BCG, the active compounds had a MBIC generally ≥ 100 µM, except for HA10Fe2 (20 µM), HA10FeCl (20-100 µM), HA10Fe3 (20-40 µM), HA10Ni2 (20 µM) and HA10Cu2 (20 µM) (Supplementary figure 1) (Tables 1–3). For the H37Ra *M. tuberculosis* strain, the active compounds had generally a MBIC ≥ 125 µM, except for HA6Ni2, HA8Ni2, HA10FeCl and HA8Fe3 with a MIC of 31.25 µM, HA10Fe3 with a MIC of 31.25-62.5 µM, HA17Fe3 with a MIC of 62.5 µM (Tables 1–3).

In order to assess whether some of the HA compounds could target PDIM biosynthesis in pathogenic mycobacteria, we investigated the susceptibility *M. bovis* BCG to vancomycin in the presence of HA10FeCl. Indeed, we previously showed that the vancomycin, usually used to treat Gram positive bacteria and inactive on pathogen mycobacteria, can target those ones when they are lacking PDIM in their cell wall [4]. Drug targeting the compounds involved in PDIM biosynthesis can thus synergize with vancomycin in the drug susceptibility assay. Interestingly, in the present study the complex HA10FeCl increased by more than 4-fold the susceptibility of *M. bovis* BCG to vancomycin in drug susceptibility assay. To investigate whether this growth inhibition results from a synergy between the HA10FeCl and the vancomycin, the Checkerboard method was also used to calculate the FICI (Table 4). The MIC of complexes HA10FeCl dropped from 46.34-92.7µg/mL to 11.59 µg/mL in the presence of vancomycin (50 µg/mL), and the MIC of vancomycin dropped from 750 µg/mL to 125 µg/mL in the presence of complexes HA10FeCl (46.35 µg/mL), suggesting that the combination can inhibit *M. bovis* BCG growth in synergy (FICI=0.292-0.417).

Table 4. Vancomycin susceptibility assay obtained in macrodilution series and analysed by the checkerboard method for *M. bovis* BCG strain. .

Compounds	MIC (µg/mL)/FICI
Vancomycin	750/-
HA10FeCl	48.18-96.37/-
HA10FeCl (46.35 µg/mL) + Vancomycin	125/0.176
Vancomycin (50 µg/mL) + HA10FeCl	11.59/0.125-0.25

-: means without calculation (it is not possible to get the FICI in the presence of only one drug in the experiment according to the equation 1).

3.2. HA10Fe2, HA12Fe2 and HA12FeCl can also reduce pre-formed P. aeruginosa biofilm.

Furthermore, in view of the large spectrum of compounds able to inhibit mycobacterial biofilm development, we investigated the anti-biofilm activity of the compounds on pre-formed *P. aeruginosa* biofilm, a well-known biofilm difficult to eradicate. Most of the compounds were totally inactive in this assay, such as HA10Ni2, HA10Cu2, HA8Cu2, $CuCl_2$, $NiCl_2$ and $FeCl_2$ even at 2.5 mM. Interestingly, the iron-complexes HA10Fe2, HA12Fe2 and HA12FeCl could inhibited the *P. aeruginosa* biofilm formation with a MBIC of 625 µM, 312.5 µM and 312.5 µM, respectively (data not shown).

3.3. Proteomic profile of the HA10FeCl-treated bacilli

In order to better understand the mode of the action of the drug candidate, we also compared the proteomics of the HA10FeCl-treated *M. bovis* BCG cells with untreated cells (Figures 1 and 2). A total 41 proteins were screened and identified with significant difference (p<0.05) by t test and with a

Preprints (www.preprints.org) | NOT PEER-REVIEWED | Posted: 4 September 2023 doi:10.20944/preprints202309.0122.v1

fold change (FC) >1.1 and <0.9, including 32 up-regulated and 9 down-regulated proteins in the HA10FeCl-treated bacilli, compared with the control without treatment (**Table S1**).

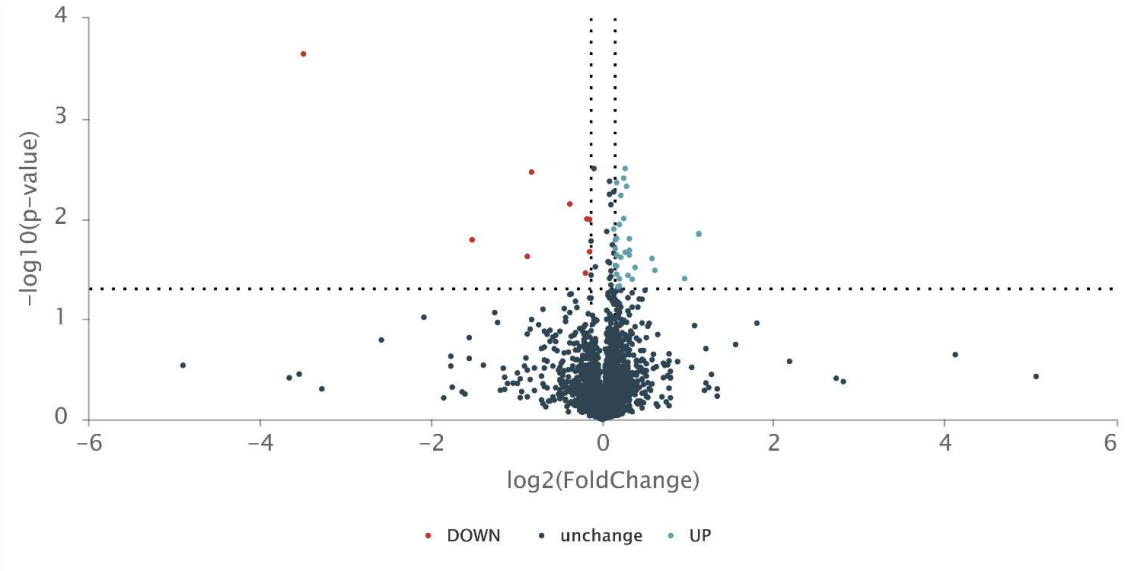

Figure 1. Proteomic analysis of the HA10FeCl-treated *M. bovis* BCG versus untreated *M. bovis* BCG control. The volcano plot of proteomic data in the HA10FeCl-treated *M. bovis* BCG compared to control. Three independent samples for each group were analysed for proteomic analysis.

Generally, the hydrolase proteins encoded by the genes (*pstC2*, *bglS*, *BCG_1059c*, *BCG_0364*, *moaC3*, *gltD*, *lipG*, *BCG_2973*, *BCG_0099*, *truA*, *BCG_1935c*, *mltG*, *topA*, *pks12*) were up-regulated. The possible membrane proteins encoded by the genes *BCG_1478*, *BCG_3932*, *BCG_3545c*, *mmpS4*, *BCG_1127c* were also up-regulated in the HA10FeCl-treated bacilli. The Phosphate transport system permease protein encoded by the gene *pstC2* with a FC of 2.19 and the Rubredoxin encoded by the *BCG_3279c* with a FC of 2.19 were also up-regulated. The proteins encoded by the genes *crgA*, *BCG_3932*, *BCG_1708*, *BCG_1384c*, *BCG_0352*, *BCG_2826*, *BCG_3492c*, *gltD*, *lipG*, *BCG_2813c*, *BCG_0099*, *BCG_1268*, *truA*, *mutT2*, *BCG_1935c*, *mltG*, *topA*, *BCG_3927*, *BCG_1127c*, *rnpA_2* were also up-regulated in HA treated *M. bovis* BCG. In addition, the proteins encoded by *pks12* (*BCG_2067c*), *BCG_2973* involved in PDIM biosynthesis and the proteins mmpS4 involved in siderophore export was also up-regulated in HA treated *M. bovis* BCG. By contrast, the proteins encoded by the genes *thiG*, *BCG_2384c* and *BCG_2177c* were down-regulated in the HA10FeCl-treated *M. bovis* BCG.

Furthermore, we also observed some up-regulated proteins, encoded *BCG_1100c*, *narK2*, *BCG_0259c*, *BCG_3092* in HA10FeCl-treated *M. bovis* BCG and down-regulated proteins, encoded by genes *PE15*, *mmpL9a* (*BCG_2361*) in the control were not identified from the proteomic profiles (data not shown).

Preprints (www.preprints.org) | NOT PEER-REVIEWED | Posted: 4 September 2023 doi:10.20944/preprints202309.0122.v1

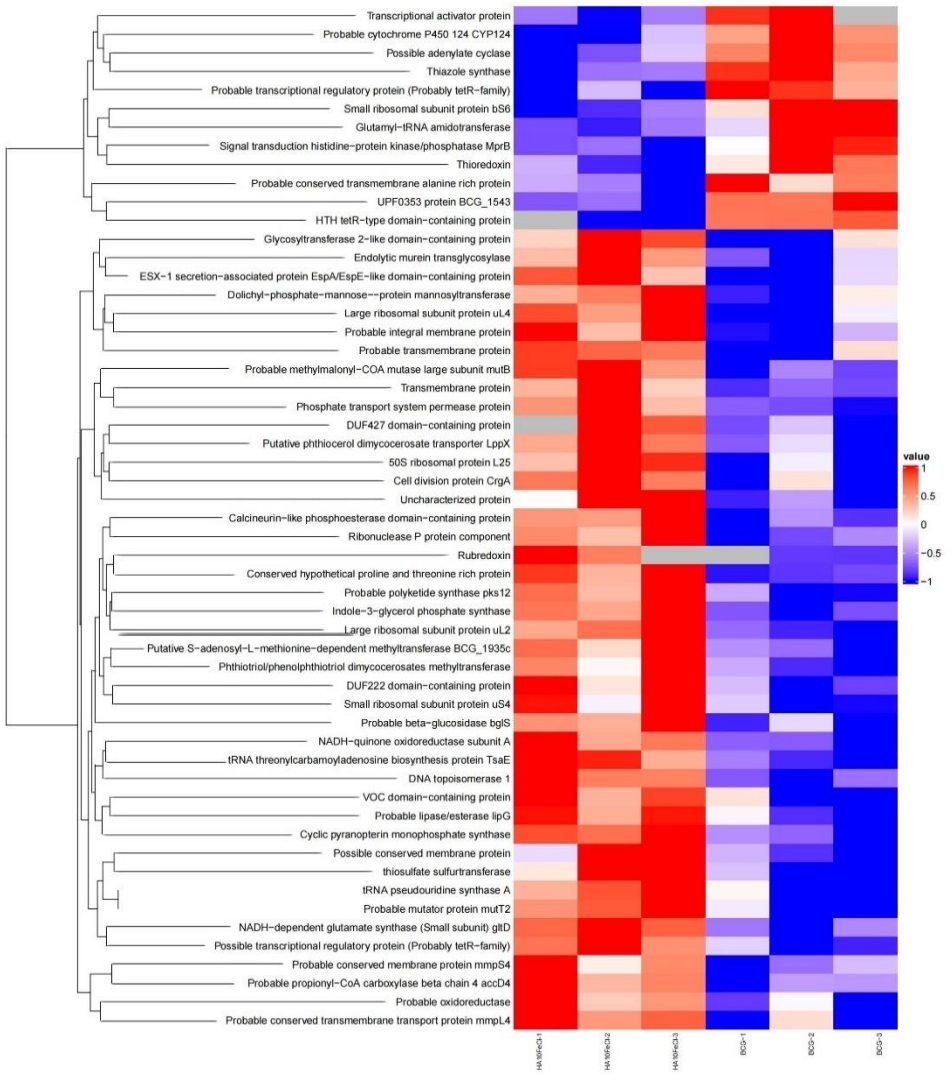

Figure 2. Proteomic analysis of the HA10FeCl-treated *M. bovis* BCG versus untreated *M. bovis* BCG control. The heatmap showing differentially expressed proteins in HA10FeCl-treated *M. bovis* BCG and control. Colours changing from blue to red indicate increased levels of proteins. Gray color indicates protein not detected in proteomic profiles. Three independent samples for each group were analysed for proteomic analysis.

4. Discussion

In the present study, the anti-mycobacterial activities and anti-biofilm activities were assessed using three mycobacteria strains (H37Ra *M. tuberculosis*, *M. bovis* BCG and *M. marinum*) and *P. aeruginosa*. Globally, the obtained results showed that HA antimycobacterial activity depended on the carbon chain length and the metal ions in the complexes. HA with C_{10} and C_{12} carbon chain (HA10 and HA12, respectively) displaying higher activity than C_2 and C_6 carbon chain HA (HA2 and HA6). Among the complexes, those with at C_8, C_{10}, and C_{12} length carbon chain, for instance, HA10FeCl, HA12FeCl, HA8Fe3, HA10Fe3 showed interesting antimycobacterial activities with MIC of 125 µM and MBIC of 31.25-62.5 µM on *M. tuberculosis*, with MBIC similar to Ni-complexes HA6Ni2 and HA8Ni2. The iron-complexes HA10FeCl, HA10Fe2, HA10Fe3 displayed higher inhibitory on *M. bovis* BCG biofilm with a MBIC of 20-100 µM, compared to the other iron-complexes. By contrast, these iron-complexes showed less activity on *M. bovis* BCG growth in planktonic conditions. Indeed, the iron-complexes inhibitory effect on mycobacteria biofilm formation is globally better than in planktonic growth conditions.

In this study our compounds were evaluated to target three mycobacterial strains, *M. bovis* BCG ($PDIM^+/PGL^+$), *M. marinum* ($PDIM^+/PGL^+$) and *M. tuberculosis* H37Ra ($PDIM^-$). As expected from a

 doi:10.20944/preprints202309.0122.v1

PDIM negative strain, the *M. tuberculosis* H37Ra strain was more susceptible to a larger panel of compounds, compared with other two mycobacterial strains. This was probably due to the impaired cell wall impermeability. As well known, the mycobacterial cell wall lipids, like trehalose monomycolate and dimycolate (TMM, TDM), PDIM, sulpholipid-1 (SL-1), diacyl trehalose (DAT), and pentacyl trehalose (PAT) are known to play an important role in pathogenesis. The proteins involved in the cell lipids biosynthesis were also considered as the potential virulence factors, like transport proteins. In *M. tuberculosis*, the mycobacterial membrane protein MmpL and MmpS family mediating transport of important cell wall lipids across the mycobacterial membrane, together with their interactor play important roles in the synthesis and export of mycobacterial outer membrane lipids [24], such as drug efflux (MmpL5 and MmpL7), siderophore export (MmpL4/MmpS4 and MmpL5/MmpS5), and heme uptake (MmpL3 and MmpL11) [25,26]. The iron–sulfur proteins [3Fe-4S] and [4Fe-4S] ferredoxins and [1Fe-0S] rubredoxins play the important role of iron-containing proteins in maintaining redox homeostasis [27]. The rubredoxin are involved in the electron transfer processes and was considered to be part of an evolutionary chain between ferredoxins and flavodoxins, might be catalyzed by cytochrome P450 (CYP) proteins [27]. It was reported that the rubredoxins transfer metabolic reducing equivalents to oxygen or reactive oxygen species and act as electron carriers in oxidative stress responses, often accompanied by inhibition of ferredoxin expression. Our results also indicate that the HA10FeCl participate the ferredoxins and flavodoxins balance in *M. bovis* BCG, by decrease the CYP124 production and up-regulated the rubredoxin to adapt the growth condition.

As well known, the virulence mycobacterial cell wall lipids PDIM and PGL, were considered as the potential targets for antituberculosis drug development. The phenolphthiocerol (phthiocerol) moiety biosynthesis of PGL (PDIM) contains several genes *ppsA-E* and *pks15/1*, encoding type I polyketide synthases (PKS), and they are highly conserved in PDIM/PGL producing mycobacteria strains, *e.g. M. tuberculosis* H37Rv, *M. bovis* BCG (Pasteur 1173P2), *M. marinum* (M strain).The *pks1* expression is also correlated with other genes, like *fadD22*, *Rv2949c*, *lppX*, *fadD29*, *pks6* and *pks12* [28]. The largest open reading frame (*pks12*) in the genome of *M. tuberculosis* H37Rv encodes probable polyketide synthase needed to produce fatty acids, probably involved in the synthesis of phthiocerol, the diol required for DIM synthesis [29]. Indeed, the phthiotriol/phenolphthiotriol dimycocerosates methyltransferase encoded by the gene BCG_2973 (Rv2952 in *M. tuberculosis*) encoded could catalyze the reduction of phthiodiolone and phenolphthiodiolone to yield phthiotriol and phenolphthiotriol in *M. tuberculosis* [30]. The proteins from the proteomic profiles encoded by the gene *pks12* and BCG_2973 were significantly up-regulated also indicated that the HA10FeCl could affect the virulent PDIM/PGL biosynthesis, further verify the sensibility of HA10FeCl to PDIM negative *M. tuberculosis* in the experimental conditions.

Additionally, the two-component regulatory system (2CRS) SenX3-RegX3 is required for *M. tuberculosis* virulence. During phosphate depletion and nutrient starvation, the phosphate-specific transport operon *pstS3-pstC2-pstA1* was induced and dependent on the (2CRS) SenX3-RegX3[29]. The disruption of the 2CRS induced the phosphate-specific transport gene *pstC2* downregulated and the phosphate-starved bacilli became phenotypically tolerant to isoniazid, further indication the role of PstC2 in stressful condition [29,30]. The up-regulated PstC2 in HA10FeCl-treated bacilli suggest that the HA10FeCl could increase the susceptibility to isoniazid and their combination could fight against the isoniazid resistant *M. tuberculosis*.

Furthermore, the proteins PE15 and MmpL9a in HA10FeCl-treated *M. bovis* BCG were not identified, probably due to the lower expression, compared with the control. As well known, the *M. tuberculosis* is surrounded by a highly impermeable outer cell wall that is composed primarily of the complex PDIM that form an outer membrane. Due to the absence of typical porins, like the β-barrel porins in Gram-negative bacteria, transports small molecules such as nutrients, metabolites, Ca^{2+} across the outer membrane need the special transporters in *M. tuberculosis*. The PE/PPE proteins were essential for Ca^{2+} efficient uptake as a specific channel[31]. Here, we observed that the PE15 was absolutely decrease in the HA10FeCl-treated bacilli from the proteomic profiles, suggesting that the PE15 could be one of the targets. The lower expression of MmpL9a (BCG_2361) in the HA10FeCl-

treated bacilli also suggested that it could be related to the linezolid resistance of the complex HA10FeCl on *M. bovis* BCG.

5. Conclusion

In summary, out of the HA and their Fe(II/III), Ni(II), Cu(II) and Zn(II) complexes evaluated for their antimycobacterial activity, the most promising growth inhibitors were some Fe(III), Cu(II) and Zn(II) complexes (HA10FeCl, HA10Fe3, HA8Fe3, HA10Zn2, HA12Cu2) which exhibited the highest antibacterial activity against pathogen mycobacteria. Their mechanisms of action showed from the proteomic profiles could be involved the cell wall lipids biosynthesis, drug resistance and tolerance, as well as siderophore metabolism. Further investigation should focus on the verification the optimal targets based on the proteomic profiles.

Author Contributions: Conceptualization: D.Y; Methodology: D.Y., I.S.S, Y.F. Z., V.F.; Resources: D.Y., R.S.L., V.F., and F. D.; Investigations: D.Y., I.S.S, N.E.M, Y.F. Z., L.-N.D., H.P.L. and G.X.C.; Formal analysis: D.Y., I.S.S, Y.F. Z.; Funding acquisition: D.Y., V.F. and R.S.L.; Supervision: V.F., F.D., M.G. and R.S.L.; Writing-original draft: D.Y. and I.S.S.; Writing-review & editing: D.Y., I.S.S. R.S.L., M.G., V.F., and F.D. All authors have given approval to the final version of the manuscript. All authors have read and agreed to the published version of the manuscript.

Funding: This research in the biological section was funded by Natural Science Foundation of Shanxi Province（20210302123356).

Conflicts of Interest: The authors declare no conflicts of interest.

References

1. W.H. Organization, Global tuberculosis report 2022, (2022).
2. M. Daffe, H. Marrakchi, Unraveling the Structure of the Mycobacterial Envelope, Microbiol Spectr 7(4) (2019).
3. C. Astarie-Dequeker, L. Le Guyader, W. Malaga, F.K. Seaphanh, C. Chalut, A. Lopez, C. Guilhot, Phthiocerol dimycocerosates of M. tuberculosis participate in macrophage invasion by inducing changes in the organization of plasma membrane lipids, PLoS Pathog 5(2) (2009) e1000289.
4. K. Soetaert, C. Rens, X.M. Wang, J. De Bruyn, M.A. Laneelle, F. Laval, A. Lemassu, M. Daffe, P. Bifani, V. Fontaine, P. Lefevre, Increased Vancomycin Susceptibility in Mycobacteria: a New Approach To Identify Synergistic Activity against Multidrug-Resistant Mycobacteria, Antimicrob Agents Chemother 59(8) (2015) 5057-60.
5. R. Kaushal, S. Thakur, K. Nehra, ct-DNA Binding and Antibacterial Activity of Octahedral Titanium (IV) Heteroleptic (Benzoylacetone and Hydroxamic Acids) Complexes, Int J Med Chem 2016 (2016) 2361214.
6. O. Bakulina, A. Bannykh, E. Levashova, M. Krasavin, Conjugates of Iron-Transporting N-Hydroxylactams with Ciprofloxacin, Molecules 27(12) (2022).
7. L.A. McAllister, J.I. Montgomery, J.A. Abramite, U. Reilly, M.F. Brown, J.M. Chen, R.A. Barham, Y. Che, S.W. Chung, C.A. Menard, M. Mitton-Fry, L.M. Mullins, M.C. Noe, J.P. O'Donnell, R.M. Oliver, 3rd, J.B. Penzien, M. Plummer, L.M. Price, V. Shanmugasundaram, A.P. Tomaras, D.P. Uccello, Heterocyclic methylsulfone hydroxamic acid LpxC inhibitors as Gram-negative antibacterial agents, Bioorg Med Chem Lett 22(22) (2012) 6832-8.
8. I.S. Sow, M. Gelbcke, F. Meyer, M. Vandeput, M. Marloye, S. Basov, M.J. Van Bael, G. Berger, K. Robeyns, S. Hermans, D. Yang, V. Fontaine, F. Dufrasne, Synthesis and biological activity of iron(II), iron(III), nickel(II), copper(II) and zinc(II) complexes of aliphatic hydroxamic acids, Journal of Coordination Chemistry 76(1) (2023) 76-105.
9. T.S. Coelho, P.C.B. Halicki, L. Silva, Jr., J.R. de Menezes Vicenti, B.L. Goncalves, P.E. Almeida da Silva, D.F. Ramos, Metal-based antimicrobial strategies against intramacrophage Mycobacterium tuberculosis, Lett Appl Microbiol 71(2) (2020) 146-153.
10. P. Gebhardt, A.L. Crumbliss, M.J. Miller, U. Mollmann, Synthesis and biological activity of saccharide based lipophilic siderophore mimetics as potential growth promoters for mycobacteria, Biometals 21(1) (2008) 41-51.
11. V. Mavrikaki, A. Pagonis, I. Poncin, I. Mallick, S. Canaan, V. Magrioti, J.F. Cavalier, Design, synthesis and antibacterial activity against pathogenic mycobacteria of conjugated hydroxamic acids, hydrazides and O-alkyl/O-acyl protected hydroxamic derivatives, Bioorg Med Chem Lett 64 (2022) 128692.

12. M.W. Majewski, S. Cho, P.A. Miller, S.G. Franzblau, M.J. Miller, Syntheses and evaluation of substituted aromatic hydroxamates and hydroxamic acids that target Mycobacterium tuberculosis, Bioorg Med Chem Lett 25(21) (2015) 4933-4936.
13. E.M. Carvalho, T. de Freitas Paulo, A.S. Saquet, B.L. Abbadi, F.S. Macchi, C.V. Bizarro, R. de Morais Campos, T.L.A. Ferreira, N.R.F. do Nascimento, L.G.F. Lopes, R. Chauvin, E.H.S. Sousa, V. Bernardes-Genisson, Pentacyanoferrate(II) complex of pyridine-4- and pyrazine-2-hydroxamic acid as source of HNO: investigation of anti-tubercular and vasodilation activities, J Biol Inorg Chem 25(6) (2020) 887-901.
14. M. Rao, D. Valentini, A. Zumla, M. Maeurer, Evaluation of the efficacy of valproic acid and suberoylanilide hydroxamic acid (vorinostat) in enhancing the effects of first-line tuberculosis drugs against intracellular Mycobacterium tuberculosis, Int J Infect Dis 69 (2018) 78-84.
15. C. Rens, F. Laval, M. Daffe, O. Denis, R. Frita, A. Baulard, R. Wattiez, P. Lefevre, V. Fontaine, Effects of Lipid-Lowering Drugs on Vancomycin Susceptibility of Mycobacteria, Antimicrob Agents Chemother 60(10) (2016) 6193-9.
16. D. Yang, G. Vandenbussche, D. Vertommen, D. Evrard, R. Abskharon, J.F. Cavalier, G. Berger, S. Canaan, M.S. Khan, S. Zeng, A. Wohlkonig, M. Prevost, P. Soumillion, V. Fontaine, Methyl arachidonyl fluorophosphonate inhibits Mycobacterium tuberculosis thioesterase TesA and globally affects vancomycin susceptibility, FEBS Lett 594(1) (2020) 79-93.
17. D. Yang, D.P. Klebl, S. Zeng, F. Sobott, M. Prevost, P. Soumillion, G. Vandenbussche, V. Fontaine, Interplays between copper and Mycobacterium tuberculosis GroEL1, Metallomics 12(8) (2020) 1267-1277.
18. S. Zeng, P. Constant, D. Yang, A. Baulard, P. Lefevre, M. Daffe, R. Wattiez, V. Fontaine, Cpn60.1 (GroEL1) Contributes to Mycobacterial Crabtree Effect: Implications for Biofilm Formation, Front Microbiol 10 (2019) 1149.
19. M. Tre-Hardy, C. Nagant, N. El Manssouri, F. Vanderbist, H. Traore, M. Vaneechoutte, J.P. Dehaye, Efficacy of the combination of tobramycin and a macrolide in an in vitro Pseudomonas aeruginosa mature biofilm model, Antimicrob Agents Chemother 54(10) (2010) 4409-15.
20. J.R. Wisniewski, A. Zougman, N. Nagaraj, M. Mann, Universal sample preparation method for proteome analysis, Nat Methods 6(5) (2009) 359-62.
21. S. Boopathi, S. Ramasamy, B. Haridevamuthu, R. Murugan, M. Veerabadhran, A.-Q. Jia, J. Arockiaraj, Intercellular communication and social behaviors in mycobacteria, Frontiers in Microbiology 13 (2022).
22. E.I. Nino-Padilla, C. Velazquez, A. Garibay-Escobar, Mycobacterial biofilms as players in human infections: a review, Biofouling 37(4) (2021) 410-432.
23. A. Viljoen, Y.F. Dufrene, J. Nigou, Mycobacterial Adhesion: From Hydrophobic to Receptor-Ligand Interactions, Microorganisms 10(2) (2022).
24. J.M. Belardinelli, C.M. Stevens, W. Li, Y.Z. Tan, V. Jones, F. Mancia, H.I. Zgurskaya, M. Jackson, The MmpL3 interactome reveals a complex crosstalk between cell envelope biosynthesis and cell elongation and division in mycobacteria, Sci Rep 9(1) (2019) 10728.
25. R. Bailo, A. Bhatt, J.A. Ainsa, Lipid transport in Mycobacterium tuberculosis and its implications in virulence and drug development, Biochem Pharmacol 96(3) (2015) 159-67.
26. K. Kurthkoti, H. Amin, M.J. Marakalala, S. Ghanny, S. Subbian, A. Sakatos, J. Livny, S.M. Fortune, M. Berney, G.M. Rodriguez, The Capacity of Mycobacterium tuberculosis To Survive Iron Starvation Might Enable It To Persist in Iron-Deprived Microenvironments of Human Granulomas, mBio 8(4) (2017).
27. T. Sushko, A. Kavaleuski, I. Grabovec, A. Kavaleuskaya, D. Vakhrameev, S. Bukhdruker, E. Marin, A. Kuzikov, R. Masamrekh, V. Shumyantseva, K. Tsumoto, V. Borshchevskiy, A. Gilep, N. Strushkevich, A new twist of rubredoxin function in M. tuberculosis, Bioorg Chem 109 (2021) 104721.
28. B. Ramos, S.V. Gordon, M.V. Cunha, Revisiting the expression signature of pks15/1 unveils regulatory patterns controlling phenolphtiocerol and phenolglycolipid production in pathogenic mycobacteria, PLoS One 15(5) (2020) e0229700.
29. T.D. Sirakova, V.S. Dubey, H.J. Kim, M.H. Cynamon, P.E. Kolattukudy, The largest open reading frame (pks12) in the Mycobacterium tuberculosis genome is involved in pathogenesis and dimycocerosyl phthiocerol synthesis, Infect Immun 71(7) (2003) 3794-801.
30. R. Simeone, P. Constant, W. Malaga, C. Guilhot, M. Daffe, C. Chalut, Molecular dissection of the biosynthetic relationship between phthiocerol and phthiodiolone dimycocerosates and their critical role in the virulence and permeability of Mycobacterium tuberculosis, FEBS J 274(8) (2007) 1957-69.
31. V. Boradia, A. Frando, C. Grundner, The Mycobacterium tuberculosis PE15/PPE20 complex transports calcium across the outer membrane, PLoS Biol 20(11) (2022) e3001906.